Supplementary Information

Cell-Mimicking Nanodecoys Neutralize SARS-CoV-2 and Mitigate Lung Injury in a Nonhuman Primate Model of COVID-19

Zhenhua Li[1,2 #], Zhenzhen Wang[1,2 #], Phuong-Uyen C. Dinh[1,2,3 #], Dashuai Zhu[1,2], Kristen D. Popowski[1,2], Halle Lutz[1,2], Shiqi Hu[1,2], Mark G. Lewis[4], Anthony Cook[4], Hanne Andersen[4], Jack Greenhouse[4], Laurent Pessaint[4], Leonard J. Lobo[5], and Ke Cheng[1,2]*

[1]Department of Molecular Biomedical Sciences and Comparative Medicine Institute, North Carolina State University, Raleigh, NC 27607, USA.

[2]Joint Department of Biomedical Engineering, the University of North Carolina at Chapel Hill and North Carolina State University, Chapel Hill, NC 27695, USA.

[3]BreStem Therapeutics Inc., Research Triangle Park, NC 27606, USA.

[4]Bioqual Inc., Rockville, MD 20852, USA.

[5]Division of Pulmonary Medicine, the University of North Carolina at Chapel Hill, Chapel Hill, NC 27599, USA.

[#]Equal Contribution

*Corresponding to: ke_cheng@ncsu.edu or ke_cheng@unc.edu

SUPPLEMENTARY METHODS

Cell culture

Human macrophage primary cells (CELPROGEN) were purchased and cultured in pre-coated flasks with human macrophage primary cell culture complete extracellular matrix (Cat# E36070-01) and media with serum (Cat# M36070-01S). Human lung spheroid cells (LSCs) and explant derived cells (EDCs) were generated from healthy whole lung donors acquired from the Cystic Fibrosis and Pulmonary Diseases Research and Treatment Center at the University of North Carolina at Chapel Hill and expanded as previously described[1,2]. Human lung tissue collection and use are approved by the IRB at the University of North Carolina at Chapel Hill and informed consent was obtained from all subjects prior to tissue collection. All procedures and experiments performed in this study involving human samples were in accordance with the ethical standards of the IRB and with the guidelines set by the Declaration of Helsinki. Human lung fibroblast cells (ATCC® PCS-201-013™) were obtained from ATCC. All procedures performed in this study involving human samples were in accordance with the ethical standards of the institutional research committee and with the guidelines set by the Declaration of Helsinki.

Immunoblotting and immunostaining

LSC and EDC cell lysates were analyzed by western blot for ACE2 (MA5-31394; Invitrogen and PA5-85139; Invitrogen) and beta-actin (MA5-15739; Invitrogen) at a 1:1000 dilution and followed by a one-hour incubation with the corresponding HRP conjugated secondary antibodies at a 1:10,000 dilution. Blots were visualized on a Bio-Rad ChemiDoc. Immunostaining was performed on cells or cryo-sectioned tissue slides fixed in 4% paraformaldehyde (PFA), which were permeabilized and blocked with Dako Protein blocking solution (DAKO; X0909) containing 0.1% saponin (47036; Sigma-Aldrich). Cells and tissues were stained with antibodies against ACE2 (MA5-31394; Invitrogen and PA5-85139; Invitrogen), SFTPC (ab3786; Abcam), Phalloidin (ab176753; Abcam), CD4 (12-0041-82, Invitrogen), CD90 (11-0909-42, Invitrogen), and CD68 (ab955; Abcam) at a dilution of 1:100-

1:200. Slides were imaged on the Olympus FLUOVIEW confocal microscope and analyzed on ImageJ (https://imagej.nih.gov/ij/).

Flow cytometry

Cells were washed with MACS flow buffer (130-091-222; MACS) and permeabilized with BD Cytofix/Cytoperm (554714; BD) prior to incubation with antibodies against ACE2 (PA5-85139; Invitrogen), EpCAM (ab71916; Abcam), CD90 (555595; BD), MUC5b (ab77995; Abcam), and vWF (ab11713; Abcam). Nanodecoys were prepared by binding the particles to 4 μm aldehyde/sulfate latex beads (A37304; Thermo Fisher) at 4°C overnight. The binding reaction was stopped by incubation of the nanodecoy-bead mixture with an equal volume of 200 nM glycine for 30 mins at room temperature followed by two washes with MACS flow buffer. Nanodecoy-bound beads were then incubated with ACE2 (PA5-85139; Invitrogen) and SFPTC (AB3786; Sigma-Aldrich) antibodies for 1 hour at 4°C followed by two washes with MACS flow buffer. The samples were then incubated with fluorescent secondary antibodies (A32731; Thermo Fisher) for 1 hour in the dark at 4°C followed by one wash with MACS flow buffer. Plain beads and unstained nanodecoy-bound beads were used as controls. Flow cytometry was performed using a CytoFlex (Beckman Coulter) or LSR-II (BD) and the data were analyzed using the FCS Express V6 (De Novo Software) or FACSDiva Software (BD).

SARS-CoV-2 stock

We expanded the SARS-CoV-2 USA-WA1/2020 stock from the BEI Resource (NR-52281; Lot #70033175; courtesy Natalie Thornburg, Centers for Disease Control and Prevention) in Vero E6 cells and harvested the virus challenge stock on day 5 following infection at 90% cytopathic effect (CPE). Full genome sequencing revealed 100% identity with the parent virus sequence (GenBank MN985325.1; courtesy David O'Connor, Shelby O'Connor, University of Wisconsin).

Histopathology and immunohistochemistry of macaques' lung tissues

Tissues were fixed in freshly prepared 4% PFA for 24 hours, transferred to 70% ethanol,

and paraffin embedded within 7 days and sectioned at 5 μm. Slides were then baked for 60 mins at 65 °C, deparaffinized in xylene, and rehydrated through a series of graded ethanol and distilled water. Subsequently, the slides were stained with hematoxylin (HSS16, Sigma-Aldrich) and eosin Y (318906, Sigma-Aldrich). An optical microscopy was used to analyze these slides. For immunohistochemistry (IHC) staining on SARS nucleocapsid protein (SARS-N), retrieval was performed in citrate buffer first (AP9003125, Thermo) and followed by treatment with 3% H_2O_2 in methanol. Slides were permeabilized and blocked with Dako protein blocking solution (X0909, DAKO) containing 0.1% saponin (47036, Sigma-Aldrich). The slides were incubated with rabbit anti-SARS-N antibody (NB100-56576, Novus, 1:200) overnight at 4 °C and then with goat anti-rabbit HRP secondary antibody (ab6721, Abcam, 1:1000) for 30 minutes. The slides were then counterstained with hematoxylin followed by bluing using 0.25% ammonia water.

Subgenomic mRNA assay

SARS-CoV-2 E gene subgenomic mRNA (sgRNA) was assessed by RT-PCR. To generate a standard curve, the SARS-CoV-2 E gene sgRNA was cloned into a pcDNA3.1 expression plasmid; this insert was transcribed using an AmpliCap-Max T7 High Yield Message Maker Kit (Cellscript) to obtain RNA for standards. Prior to RT-PCR, samples collected from challenged animals or standards were reverse-transcribed using Superscript III VILO (Invitrogen) according to the manufacturer's instructions. A Taqman custom gene expression assay (ThermoFisher Scientific) was designed using the sequences targeting the E gene sgRNA. Reactions were carried out on a QuantStudio 6 and 7 Flex Real-Time PCR System (Applied Biosystems) according to the manufacturer's specifications. Standard curves were used to calculate sgRNA in copies per mL or per swab; the quantitative assay sensitivity was 50 copies per mL or per swab.

RNAscope in situ hybridization

RNAscope in situ hybridization was performed using SARS-CoV-2 anti-sense specific

probe v-nCoV2019-S (ACD Cat. No. 848561) targeting the positive-sense viral RNA, SARS-CoV-2 sense specific probe vnCoV2019-orf1ab-sense (ACD Cat. No. 859151) targeting the negative-sense genomic viral RNA, and ZIKA probe V-ZIKVsph2015 (ACD Cat. No. 467871) as a negative control. Briefly, slides were deparaffinized in xylene first and then rehydrated through a series of graded ethanol to distilled water followed by incubating with RNAscope® H_2O_2 (ACD Cat. No. 322335) for 10 mins at room temperature, retrieval was performed for 15 mins in ACD P2 retrieval buffer (ACD Cat. No. 322000) at 95-98 °C, followed by treatment with protease plus (ACD Cat. No. 322331) for 30 min at 40 °C. Probe hybridization and detection were developed using the RNAscope® 2.5 HD Detection Reagents-RED (ACD Cat. No.322360) according to the manufacturer's instructions.

Immunofluorescence staining of macaques' lung tissues

In brief, the pretreatment of slides is the same with IHC assay including dewaxing, rehydration, retrieval and 3% H_2O_2 treatment. After that, slides were first blocked with 5 % BSA for 30 mins followed by rinse in PBS buffer. Primary rabbit anti-SARS-N antibody (1:200) incubated overnight at 4 °C and then goat anti-rabbit Alexa Fluor® 594 (Abcam, ab150080, 1:500), AF-488-CD206 (Santa Cruz Biotechnologies, sc-376108, 1:150), eFluor 660-CD68 (eBioscience, 50-0681-82, 1:200) and Alexa Fluor® 568-Iba-1 (Abcam, ab221003, 1:200) were incubated at RT for 1 hr. For co-localization assay, the FITC-pan-CK (abcam, ab78478, 1:200) was incubated at RT for 1 hr after the incubation of SARS-N. All slides were imaged using an Olympus FLUOVIEW confocal microscope.

References

1. Dinh, P.-U. C. *et al.* Inhalation of lung spheroid cell secretome and exosomes promotes lung repair in pulmonary fibrosis. *Nat. Commun.* **11**, 1064 (2020).
2. Cores, J. *et al.* A pre-investigational new drug study of lung spheroid cell therapy for treating pulmonary fibrosis. *Stem Cells Transl. Med.* (2020). doi:10.1002/sctm.19-0167

SUPPLEMENTARY FIGURES

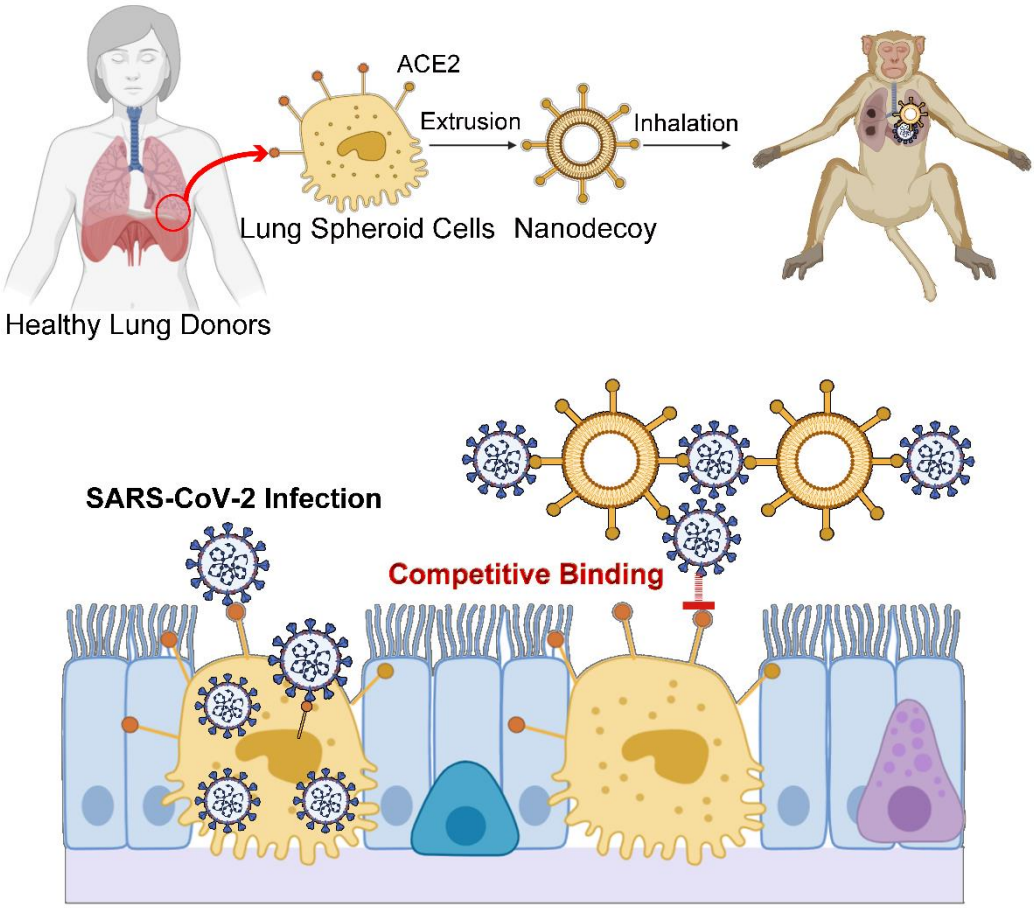

Figure S1. Schematic illustrating the generation of nanodecoys from lung spheroid cells and nanodecoy therapy for SARS-CoV-2 infection. Created with BioRender.com.

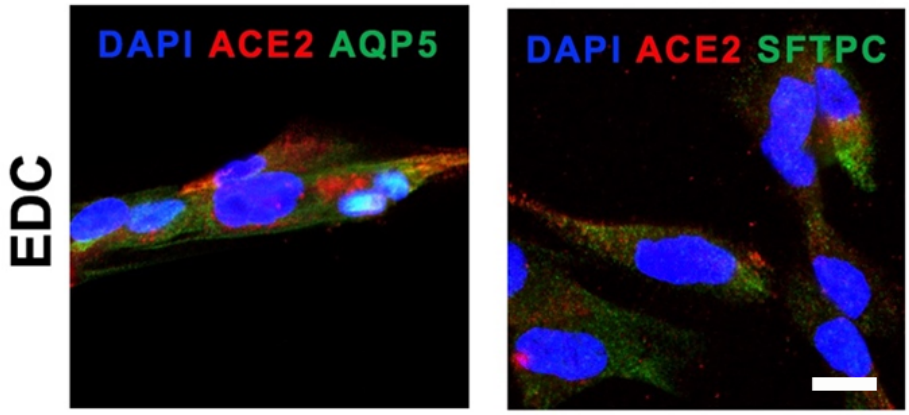

Figure S2. Confocal images showing lung explant derived cells (EDCs) labeled with ACE2, AQP5, and SFTPC antibodies. Scale bar, 20 μm.

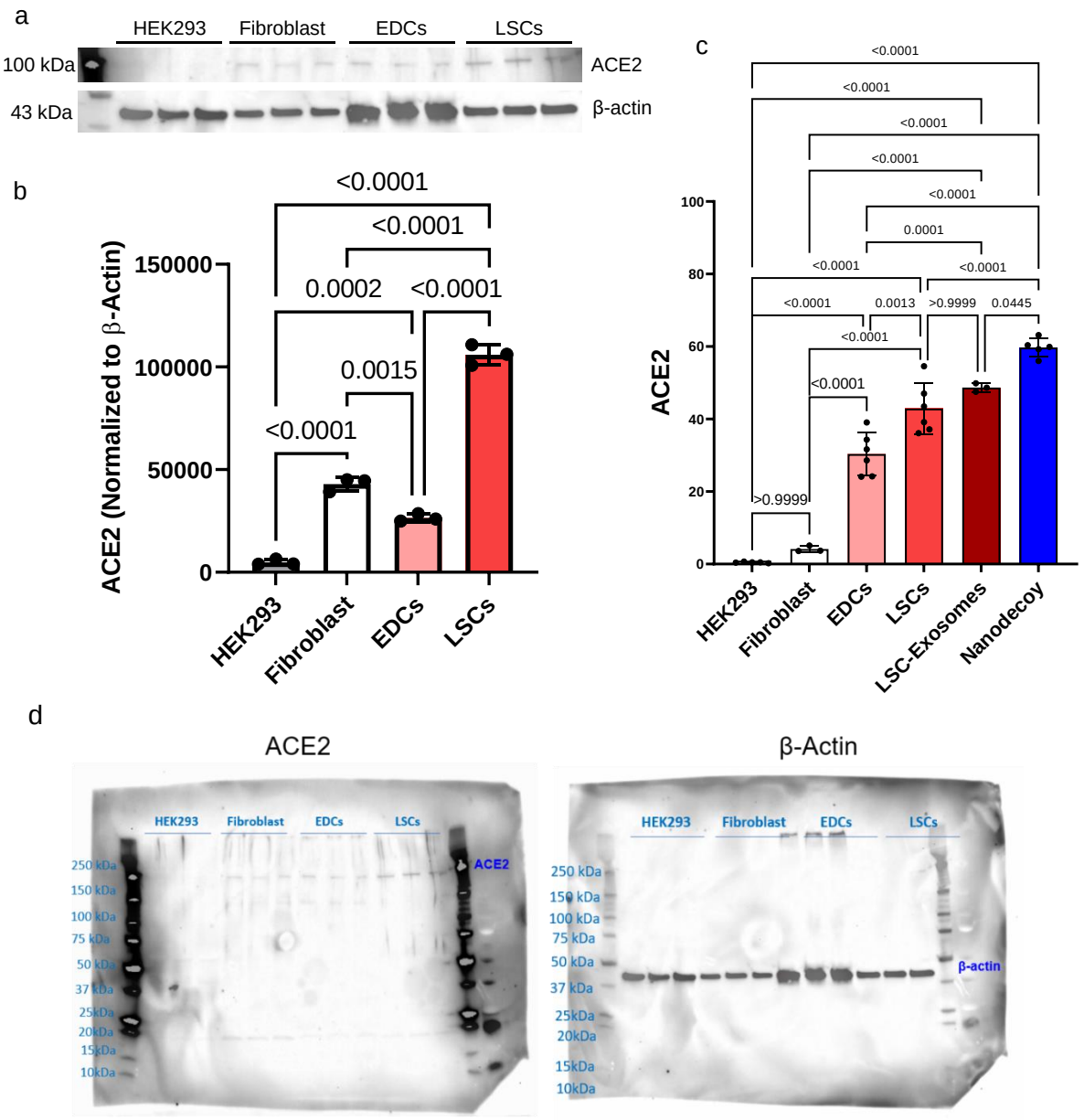

Figure S3. Immunoblotting and flow cytometry of HEK293 cells, human fibroblasts, human lung explant-derived cells (EDCs) and human lung spheroid cells (LSCs) for ACE2 expression. (a) Western blots of HEK293, human lung fibroblasts, EDCs, and LSCs. (b) Quantitative results from (a). Data are shown as mean ± SD, *n*=3 independent experiments. (c) Flow cytometry analysis of ACE2 positive percentages in HEK293 cells, human lung fibroblasts, EDCs, LSCs, LSC-Exosomes and LSC-nanodecoys. Data are shown as mean ± SD, *n*=3 or 6 independent experiments. (d) Unprocessed western blots images from (a).

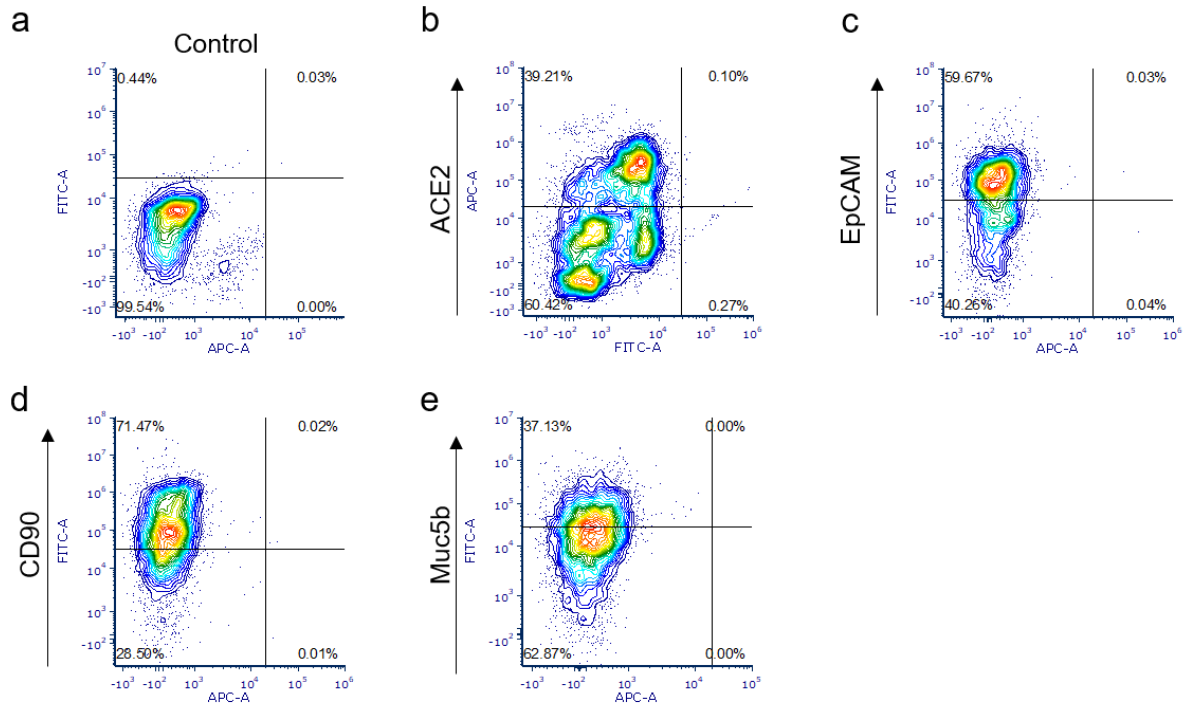

Figure S4. Flow cytometry characterizations of human LSCs. See Supplementary Figure S17 for gating strategies.

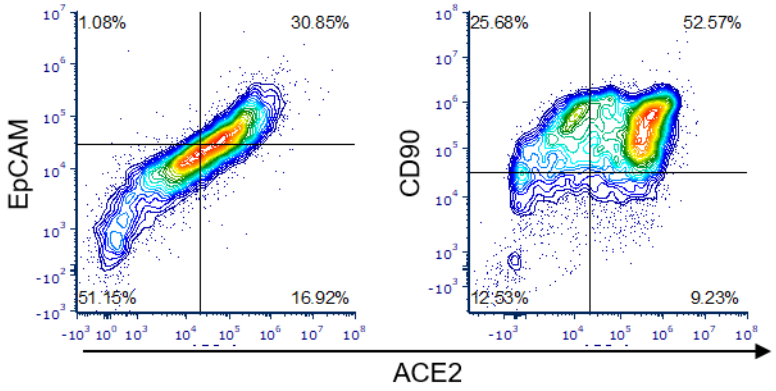

Figure S5. **Double-stain flow cytometry characterizations of ACE2^{+} LSCs.** See Supplementary Figure S17 for gating strategies.

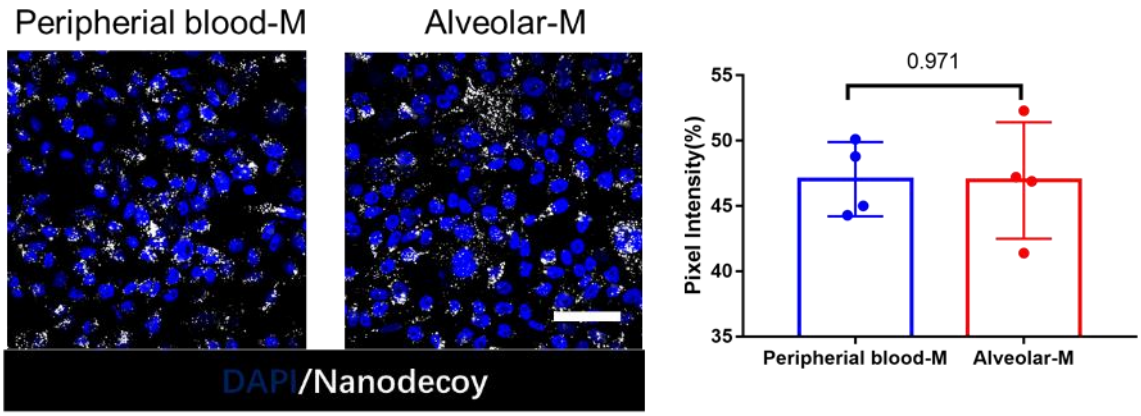

Figure S6. Internalization of nanodecoys by macrophages. Left, representative confocal images showing internalization of nanodecoys by macrophages derived from peripheral blood or lung tissues. Right, quantitative results on nanodecoy internalization**.** Data are shown as mean ± SD, *n* = 4 independent experiments. Scale bar, 50 μm.

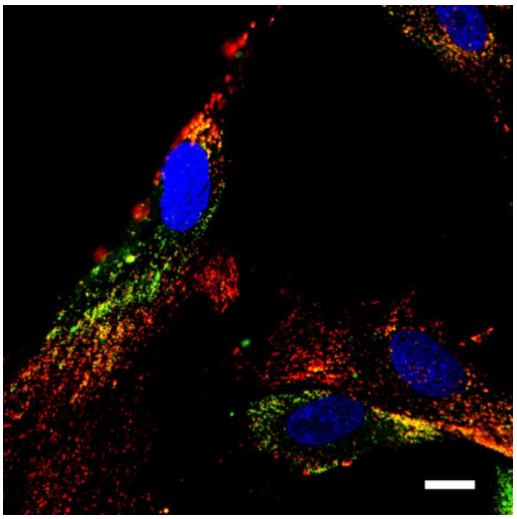

Figure S7. A representative confocal image showing SARS-CoV-2 mimic internalized by LSCs. Scale bar, 20 μm.

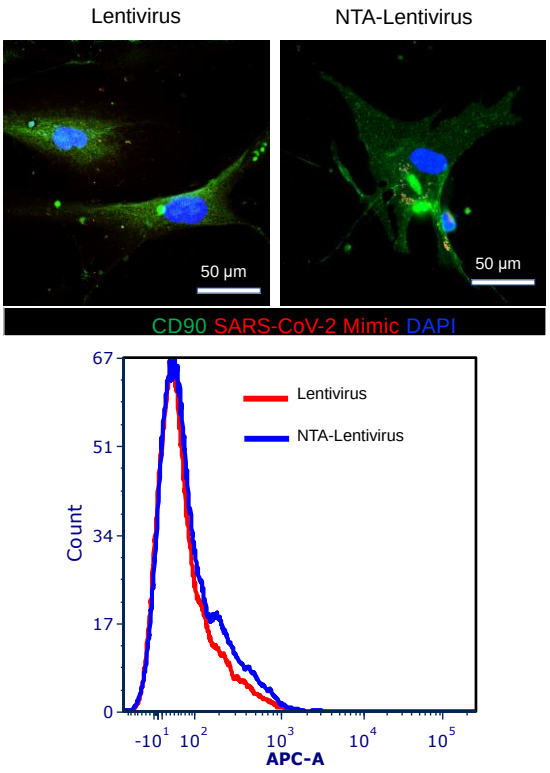

Figure S8. **Confocal imaging (upper panel) and flow cytometry analysis (lower panel) showing internalization of lentivirus and NTA-tagged lentivirus was not different.** See Supplementary Figure S18 for gating strategies.

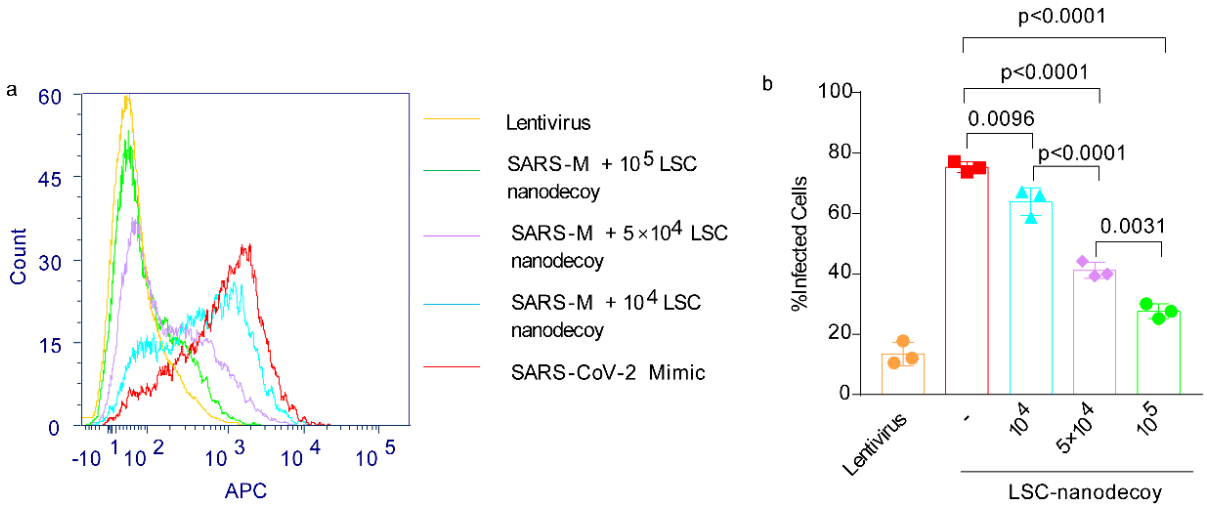

Figure S9. Nanodecoys block viral entry of SARS-CoV-2 mimics. (a) Flow cytometry analysis showing that the nanodecoys blocked virus entry into lung cells in a dose-dependent manner and (b) corresponding quantitative results from (a). Data are shown as mean ± SD, *n*=3 independent experiments. Statistical analysis was performed with one-way ANOVA and a Tukey post hoc test. See Supplementary Figure S18 for gating strategies.

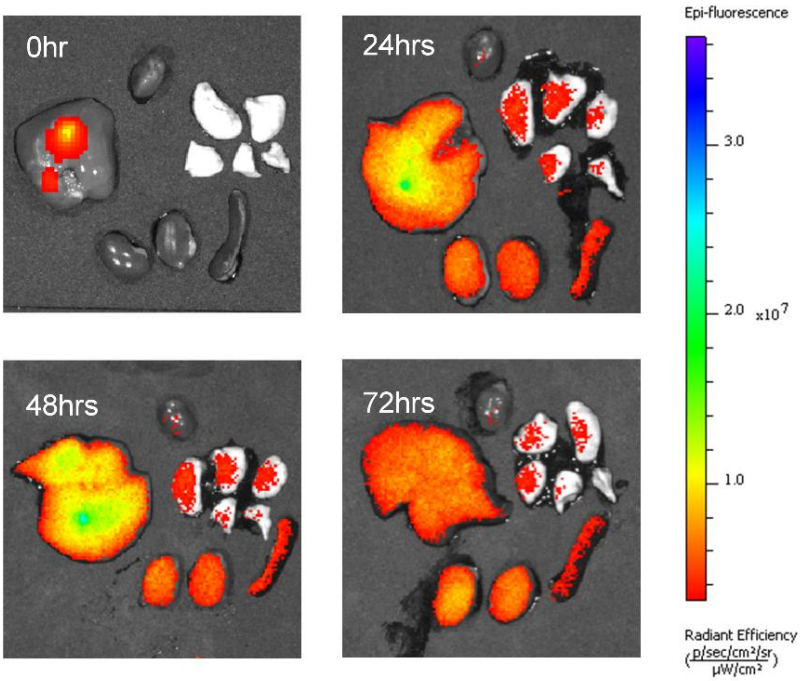

Figure S10. Biodistribution of inhaled nanodecoys. Ex vivo fluorescent images of major organs at various time points after inhalation of LSC-nanodecoys.

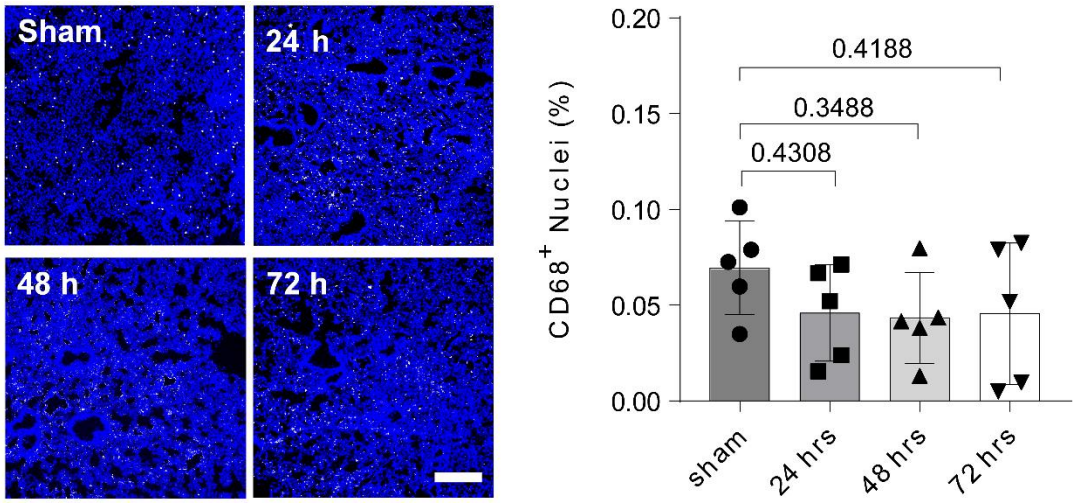

Figure S11. Nanodecoy inhalation does not trigger inflammation in the lungs. Left, confocal images showing CD68 positive cells in lung tissues at various time points after inhalation of LSC-nanodecoys. Right, quantitative results from images on the left. Data are shown as mean ± SD, *n*=3 animals per group and five images were taken per group. Statistical analysis was performed by one-way ANOVA with a Tukey post hoc test. Scale bar, 200 μm.

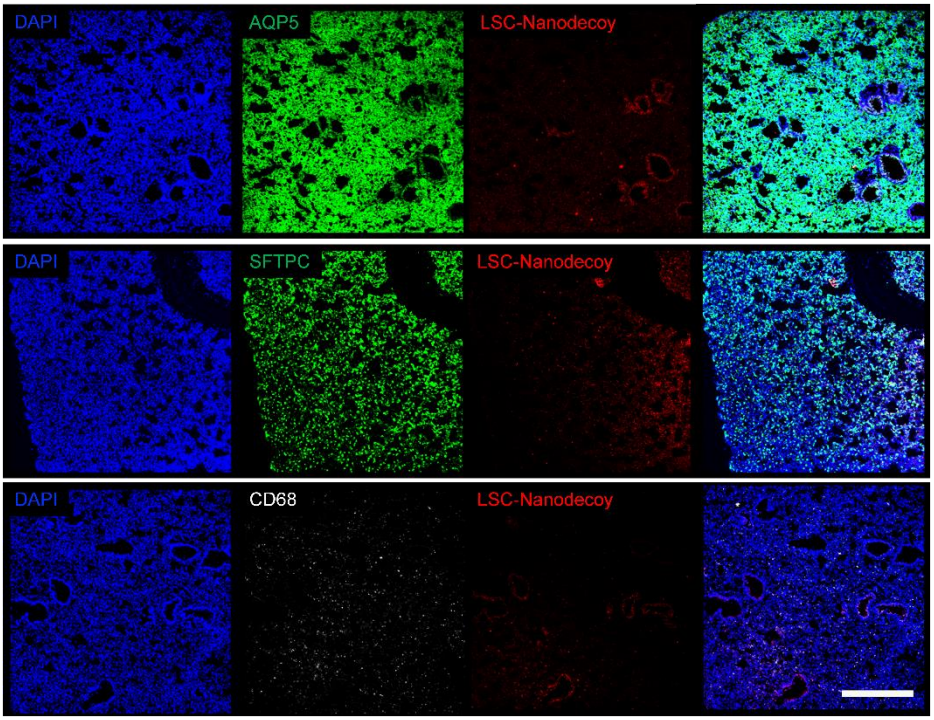

Figure S12. Unmerged images for Figure 5D. Representative confocal images showing LSC-nanodecoys in lung tissues co-localizing with lung cells (AQP5, SFTPC) and macrophages (CD68) 24 hrs post-inhalation. Scale bar, 200 μm.

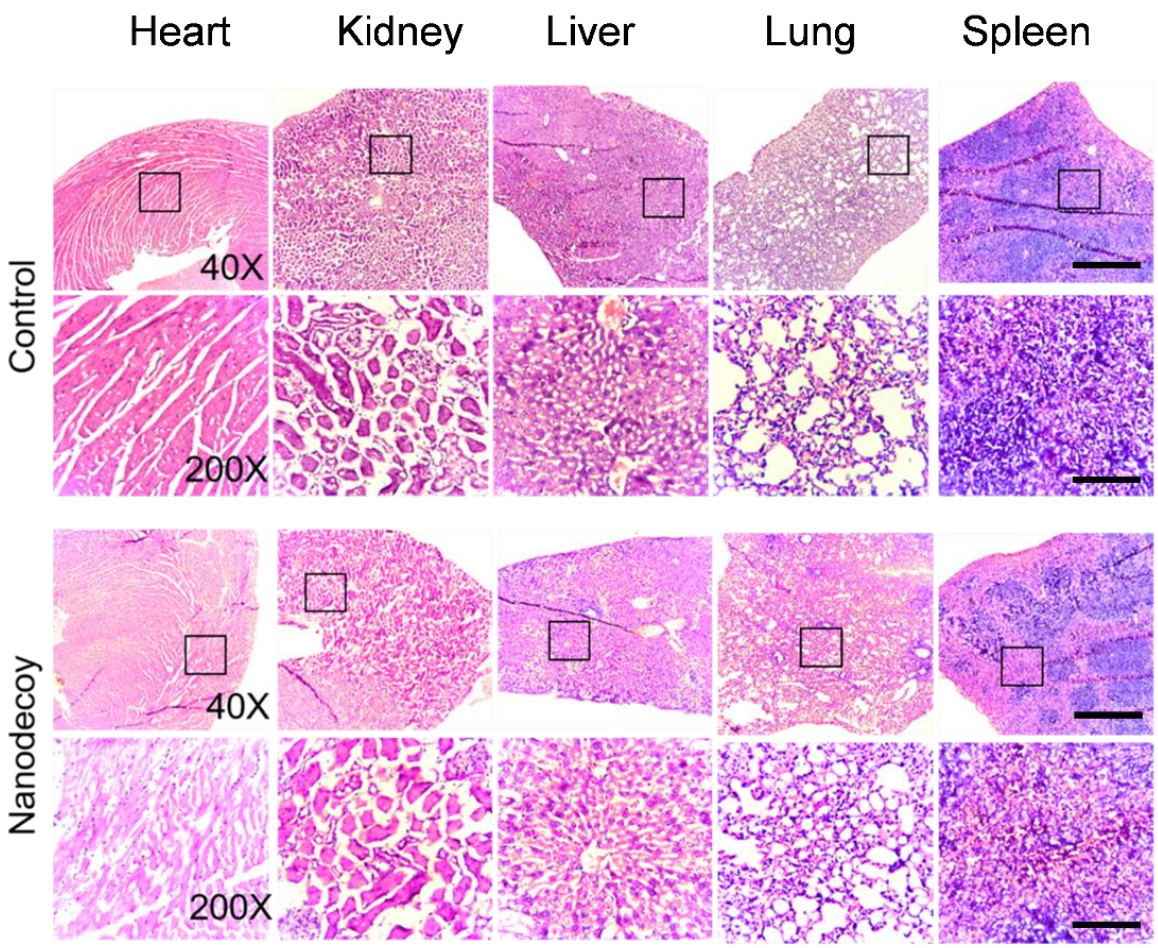

Figure S13. Pathological studies on the toxicity of LSC-nanodecoy inhalation therapy. H&E staining of major organs 14 days after LSC-nanodecoy treatment. Scale bars, 560 μm (40× images) and 110 μm (200× images).

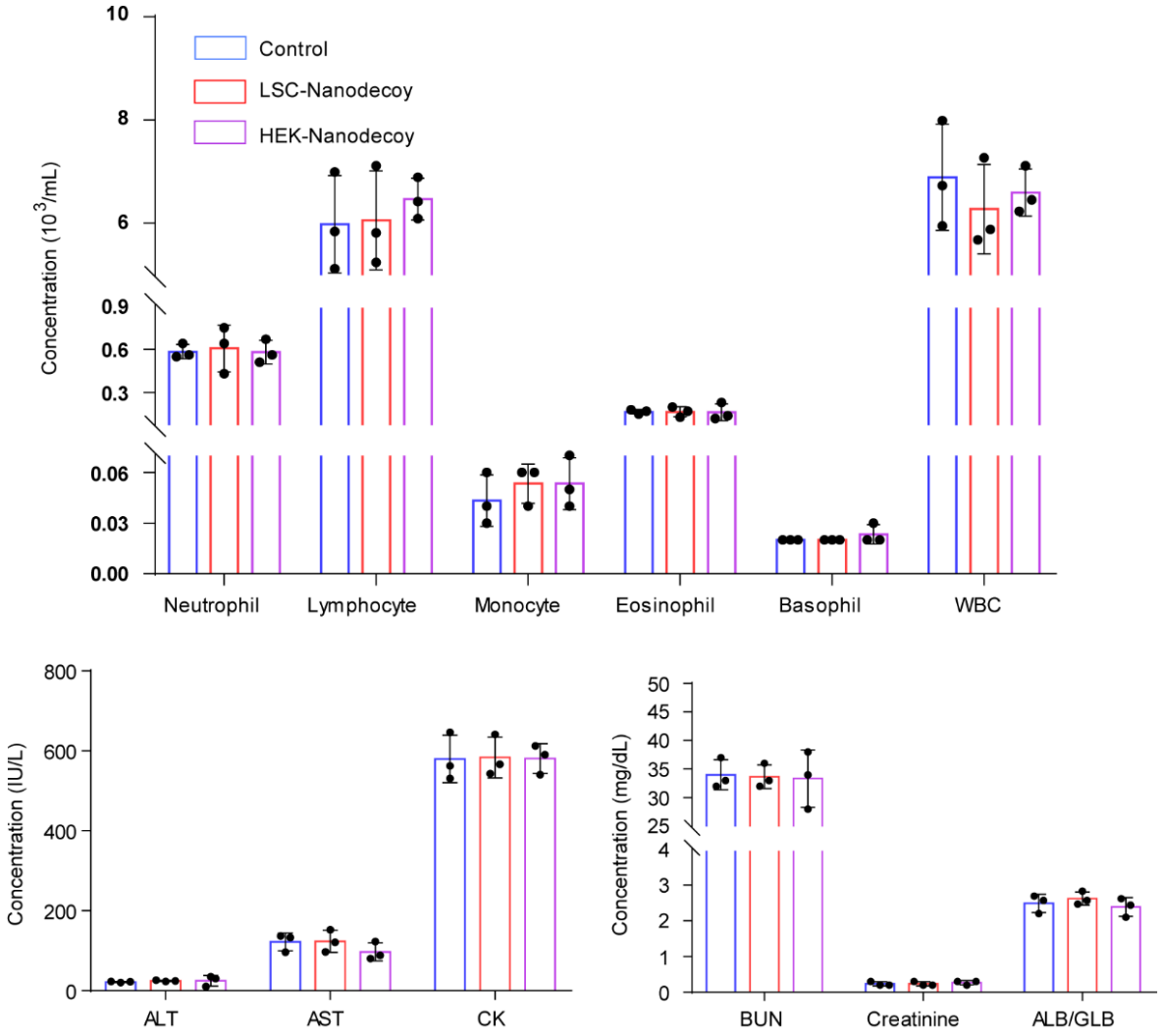

Figure S14. Hematology and biochemistry studies on nanodecoy toxicity in mice 14 days after inhalation. Data are shown as mean ± SD, *n*=3 animals per group.

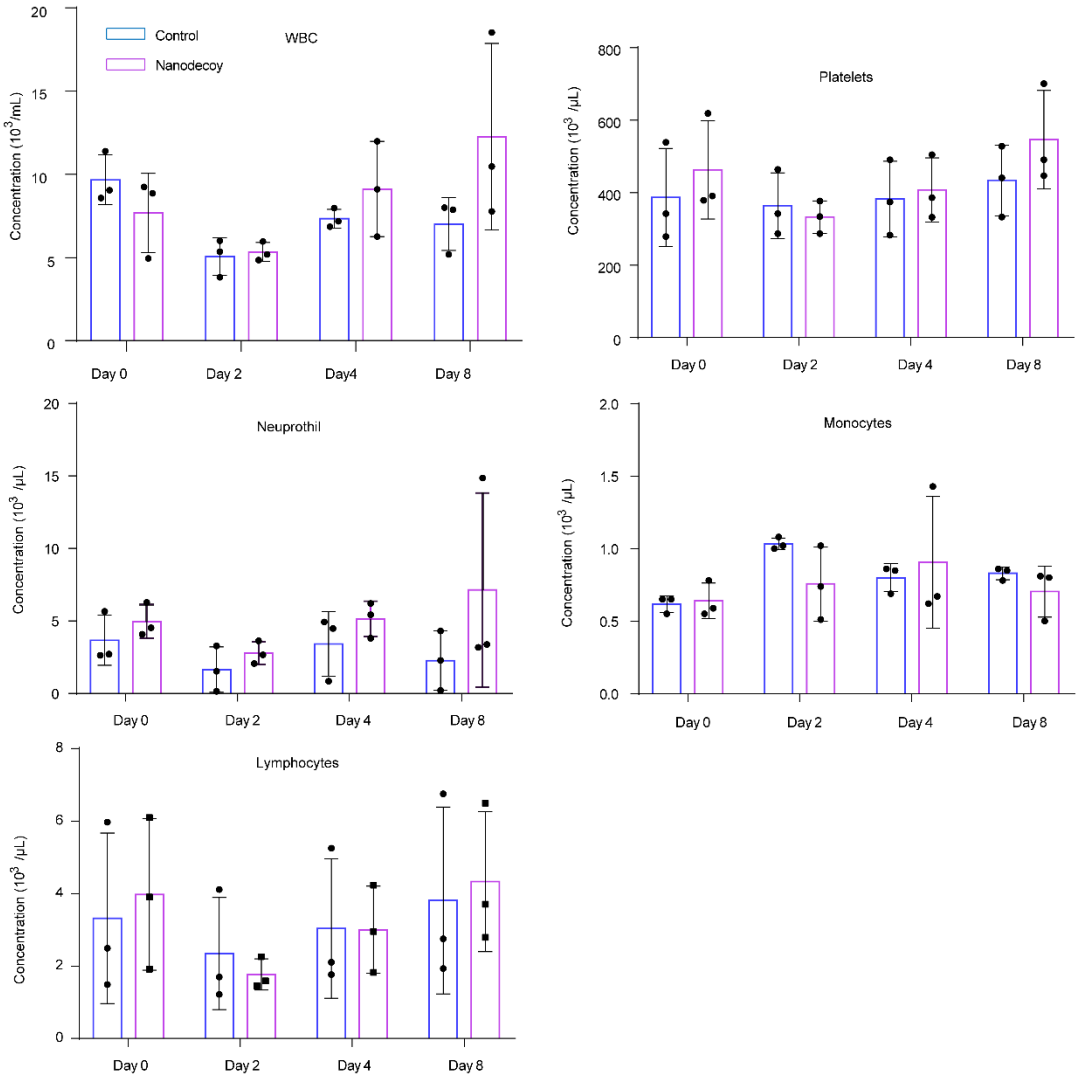

Figure S15. Hematology studies in cynomolgus macaques after LSC-nanodecoy therapy.

Data are shown as mean ± SD, *n*=3 animals per group.

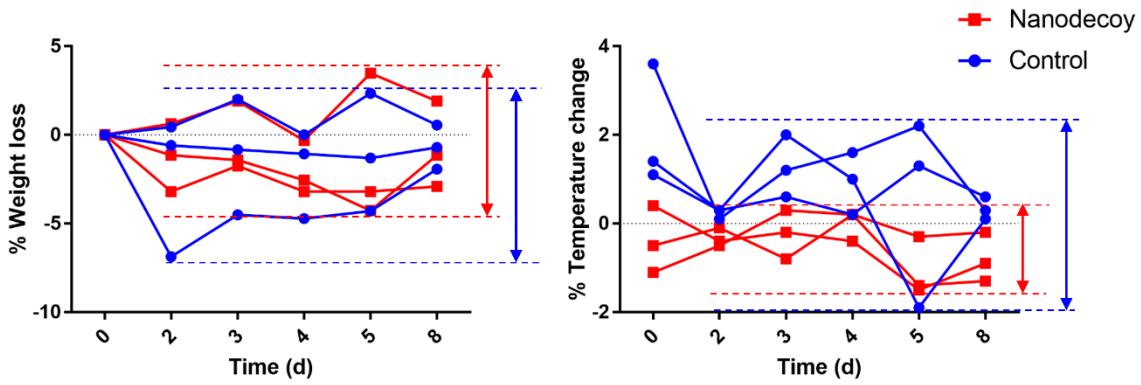

Figure S16. Percent of weight and temperature changes after SARS-CoV-2 challenge in individual cynomolgus macaques. *n*=3 animals per group.

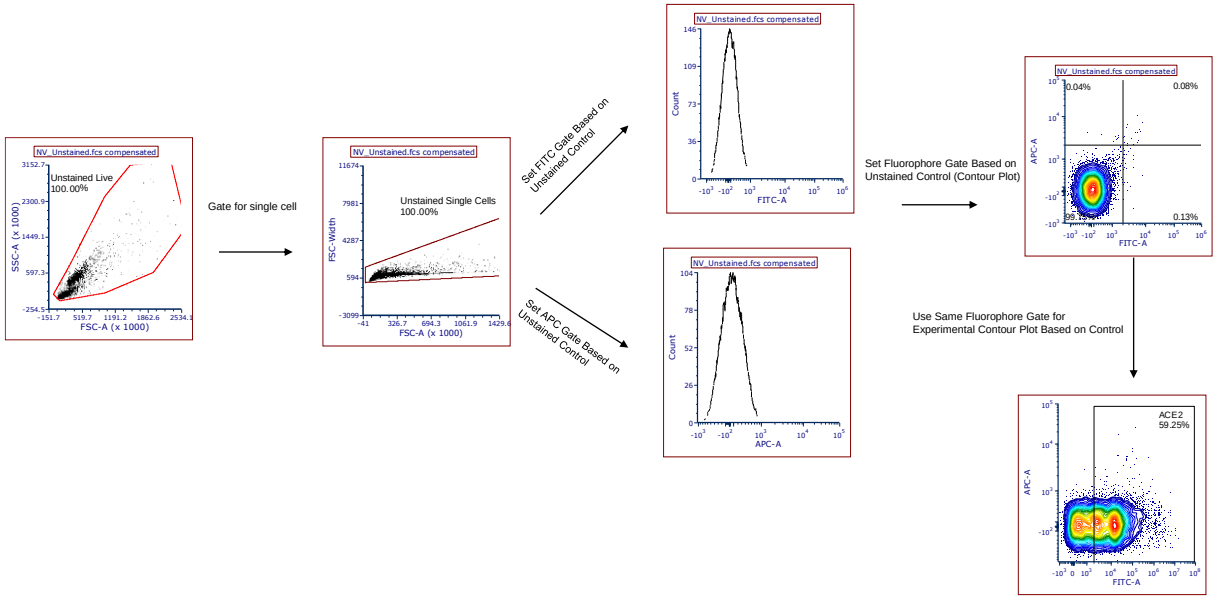

Figure S17. Flow cytometry gating strategies for experiments in Figures 1b, c, g, h, and Supplementary Figures S4 and S5.

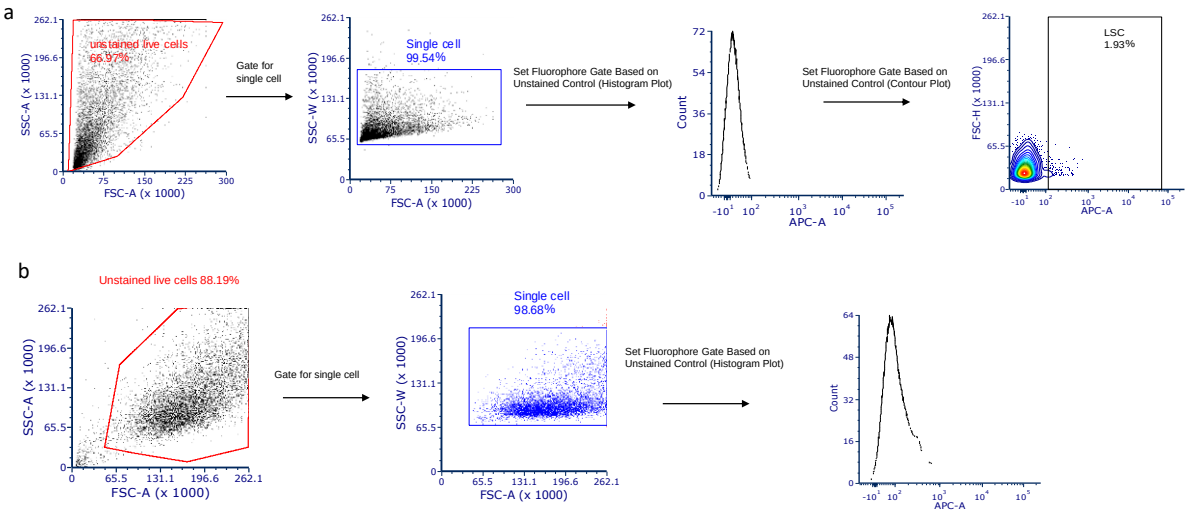

Figure S18. Flow cytometry gating strategies for experiments in Figures 2i-l (a) and Figures 3m-n (b), and Supplementary Figure S8 (b) and S9 (b).